

Student Name: Matthew Packer**Date:** 08/07/2015**Project Title:** Chemoradiosensitization of Malignant Glioma through Co-inhibition of Redundant DNA Repair Pathways**Primary Supervisor Name and Department:**

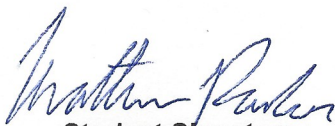
Dr. Sachin Katyal, Department of Pharmacology & Therapeutics

Co-Supervisor Name and Department:

Dr. Magimairajanlssai Vanan, Department of Biochemistry & Medical Genetics

SUMMARY: (no more than 250 words single spaced)

Malignant glioma (MG), the most common human primary brain tumour, is a cancer that has long thwarted attempts to ameliorate its devastatingly high mortality rate. Redundant DNA repair pathways confer on MG a great degree of drug resistance that contemporary treatment regimens are unable to sufficiently overcome. ATM, TDP1, PARP-1, and DNA-PKcs are important molecules of DNA repair that enable MG to mend DNA strand breaks induced by chemotherapy and radiation that would otherwise be specifically lethal to these tumours. In the present study, we have assessed the effects of inhibition of these repair molecules in the treatment of MG. We have shown that a combinatorial strategy of co-inhibition of repair molecules chemoradiosensitizes MG, markedly amplifying therapeutic response. Dual genetic knockdown of ATM and TDP1 and chemical co-inhibition of ATM and PARP-1 both curtailed DNA single strand break repair, significantly augmenting the genotoxic damage incurred by MG cells using the Topoisomerase-1 inhibitor, camptothecin, and ionizing radiation. Furthermore, co-inhibition of these repair molecules results in deficiencies in MG DNA damage repair rate, decreased tumour cell proliferation, and an escalated cytotoxic response of MG to therapy. Targeting these DNA damage repair molecules will allow existing anti-cancer therapeutic strategies to more specifically kill MG cells by lowering the chemoradiotherapeutic threshold of tumour cell genotoxicity through co-inhibition of redundant repair pathways, thus reducing off-target effects. My findings have the potential to lead to better MG treatment strategies that enhance therapeutic efficacy, patient survival, and quality-of-life.

**Student Signature**

Matthew Packer

ACKNOWLEDGEMENTS:

I gratefully acknowledge the support by one or more of the following sponsors;

CancerCare MB

H.T. Thorlakson Foundation

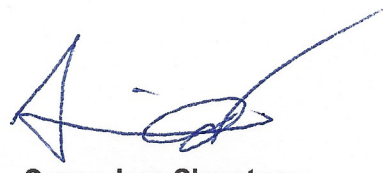
Dean, College of Medicine

Research Manitoba

Children's Hospital Research Institute of MB

Kidney Foundation of Manitoba

Other:

**Supervisor Signature**

Sachin Katyal

Manitoba Medical Service Foundation

Associate Dean (Research), College of

Medicine

Heart and Stroke Foundation

Health Sciences Centre Research

Foundation

Introduction and Background:

Glioma refers to a spectrum of primary central nervous system tumours arising from glial cells. The focus of this study is a subtype known as glioblastoma multiforme (also referred to as malignant glioma, MG), which is a Grade IV astrocytoma[1], and the most common and aggressive human primary brain tumour, afflicting individuals of all ages[2]. MG prognoses are generally poor and the disease is rarely curable, with median adult survival of 14 months[3, 4] and a 98% three-year mortality rate on standard treatment from time of diagnosis[5]. Medical intervention, which involves surgical resection and post-operative radiotherapy with adjuvant chemotherapy, is highly invasive, and incurs neurocognitive trauma and impairment. Despite these treatments, tumour recurrence occurs in over 90% of afflicted patients[6]. Numerous chemotherapeutic regimens have been assessed in hope of improving therapeutic efficacy, but there has been little success[7]. The impenitent stealth of patient death from MG is devastating to families and the community-at-large.

Glioma tumorigenesis is characterized by unstable cell proliferation, which results in the accumulation of chromosomal rearrangements. While some of these rearrangements serve to enhance the intrinsic cellular DNA repair process and counteract genotoxic treatment efforts, they often also produce defects in specific DNA repair pathways, resulting in the induction of additional compensatory or redundant repair pathways in tumour cells in response to genotoxic stress. As a result of these defects, tumours increase the activity of and become more dependent on redundant DNA repair pathways, which enhances resistance to front-line conventional DNA damaging radio- and chemotherapy, thus increasing off-target effects and toxicity[8, 9]. However, counteracting these essential pathways offers the greatest potential as tumour-specific therapeutic targets[10]. Consequently, progress to further ameliorate outcomes of MG patients requires a better understanding of tumour DNA repair biology to supplement existing cancer treatment strategies.

In addition to their defects in DNA repair pathways, MG cells are characterized by cell cycle checkpoint deficiencies which shorten the duration of the transient cell cycle arrest period that is available for DNA repair relative to that of normal cells[11]. As a result, while there is still sufficient time for near complete repair to occur in the absence of pathway inhibition, inhibitors of DNA repair may preferentially sensitize brain cancer cells to DNA damaging therapeutic modalities, thereby allowing treatment to take full advantage of glioma's reliance on redundant repair pathways.

Ataxia telangiectasia mutated (ATM), DNA-PK catalytic subunit (DNA-PKcs), Poly(ADP-ribose) polymerase-1 (PARP-1), and Tyrosyl-DNA phosphodiesterase 1 (TDP1) are four integral molecules of DNA repair for which targeted inhibitors have been developed (Fig. 1). These repair molecules resolve two classes of DNA strand breaks, single-strand breaks (SSBs) and double-strand breaks (DSBs), by specific dedicated SSB repair (SSBR) and DSB repair (DSBR) pathways[12, 13]. The inability to properly process and repair the more frequently occurring SSBs can interfere with the DNA replication and transcription machinery, resulting in persistent SSBs, formation of the particularly genotoxic DSB lesions, and a variety of cellular pathologies, including senescence, cancer, and death.

Coordinate inhibition of ATM and DNA-PKcs targets the DSBR pathway (Fig. 1A):

ATM is a key serine/threonine protein kinase required for coordination of apoptosis and cell cycle checkpoint activation for arrest and repair following DNA damage. While its major activity is in orchestration of the DNA DSB response, ATM has been shown to have a secondary role in the prevention of nervous system SSB accumulation (Fig. 2). ATM carries out selective

substrate phosphorylation of a number of downstream repair molecules, such as p53 and Chk2. In association with the MRN complex, inactive ATM, which exists as a dimer, autophosphorylates on serine 1981, forming the active phospho-ATM monomer. Mutation of ATM results in ataxia telangiectasia, a heritable childhood disease marked by severe neurodegeneration, immunodeficiency, radiosensitivity, and predisposition to malignancy[14]. Previous studies have shown that ATM deficient cells show proliferation defects, G1 checkpoint dysfunction, early senescence, and high sensitivity to oxidative and topoisomerase-1 stress, making ATM a promising target for DNA repair inhibition in the treatment of cancer[15].

Similar to ATM, DNA-PKcs is a nuclear serine/threonine kinase which is recruited to DSBs for the protection of broken ends and further recruitment of other repair proteins, ultimately resulting in DNA end-ligation by means of the non-homologous end joining (NHEJ) pathway. DNA-PKcs has been shown to cooperate with ATM, and the two may have some functional redundancy, as only dual inactivation of DNA-PKcs and ATM appears to be lethal during embryogenesis[16].

Coupled inhibition of PARP-1 and TDP1 suppresses activity of the SSBR pathway (Fig. 1B):

PARP-1's major DNA repair function is in base excision repair of SSBs, but it is also involved in a subtype of NHEJ for repair of DSBs. As it is located upstream of TDP1 in the SSBR pathway, PARP-1 inhibition is anticipated to have some effect overlap with TDP1 inhibition. PARP-1 functions to recruit repair factors along with XRCC1[17]. Its inhibition may increase DSBs by preventing SSBR, and thus leading to the collapse of stalled replication forks.

TDP1 is also a molecule involved in DNA SSBR. In the nervous system, TDP1 has essential roles in resolution of Topoisomerase 1 cleavage complex (Top1-cc) lesions, which are transient intermediates during DNA transcription and replication formed by action of topoisomerase 1 (Top1) to relieve DNA torsional stress [18]. TDP1 cleaves and processes the Top1-DNA complex phosphodiester bond as well as oxidative damage DNA lesions, repairing altered 3' DNA ends. TDP1 mutation occurs in the childhood neurodegenerative syndrome spinocerebellar ataxia with axonal neuropathy-1 (SCAN1), characterized by late onset progressive cerebellar degeneration as well as peripheral neuropathy, hypoalbuminemia, and hypercholesterolemia. Mouse knockout experiments have shown that TDP1 is required in primary neural cells for the rapid repair of SSBs induced by ionizing radiation and Top1 inhibition[19].

Co-inhibition of ATM and TDP1 impedes DSBR, SSBR, and Top1-cc resolution (Fig. 2):

We have previously found that both ATM and TDP1 are of critical importance in the coordination of DNA SSBR, as co-ablation of these gene products during embryogenesis results in substantial accumulation of the genotoxic Top1-cc lesions in replicating neuroprogenitors, inducing pronounced DNA damage and p53-mediated cell apoptosis, thus resulting in early embryonic lethality[20]. These findings are significant considering the antagonistic effects of TDP1 on Top1-cc formation, which reduces the efficacy of Top1 poisons such as the camptothecin (CPT) cohort of anti-tumorigenic Top1 inhibitors. CPT induces DNA breaks by prolonging the half life of Top1-cc's, thereby increasing the likelihood of their conversion into SSBs. Top1-cc's are normally very short lived, but collision with replication forks or machinery and trapping by proximal oxidative DNA breaks can result in their conversion to Top1-linked DNA breaks, accumulation of which ultimately leads to cell death[21]. While Top1-cc's do form DSBs, more than 95% of Top1-linked DNA breaks are SSBs, and studies have shown that, unlike DSBs, deficient SSBR leads almost exclusively to neuropathology in the absence of extraneurological phenotypes, accounting for the relevance of SSBs to glioblastoma[22]. Ionizing radiation induces oxidative breaks, with a higher proportion of DSBs to SSBs, but also stabilizes nearby Top1-cc's, thereby indirectly inducing Top1-associated SSBs.

In this study, we show that co-inhibition of ATM, TDP1, PARP-1, and DNA-PKcs has the ability to sensitize MG to the Top1-associated lesions produced by chemotherapy and radiation, lowering the genotoxic threshold of tumour cells through inhibition of redundant repair pathways. Supported by genetic techniques, my findings show that the use of targeted chemical inhibitors of DNA repair has the potential to augment therapeutic efficacy while minimizing neural and systemic side effects in the treatment of glioblastoma multiforme.

Materials and Methods:

Cell line culturing:

The well-defined U-87 MG cell line was maintained in DMEM (Dulbecco's Modified Eagle's Medium) complete medium (10% FBS, 1× glutamax, 100 U/ml penicillin, 100 µg/ml streptomycin, all from Gibco). Cells were subcultured at a 1:10 dilution approximately once every three days.

Short-hairpin RNA generation of ATM/TDP1 knockdowns:

Lentivirus particles were used to deliver and express shRNAs to knockdown human ATM (shATM) and TDP1 (shTDP1), with a non-target scrambled shRNA (shSCM) used as a control. All MISSION shRNA plasmid DNA constructs were obtained from Sigma-Aldrich. Three days following lentiviral transduction, cells underwent puromycin selection (1 µg/ml) to establish stable knockdown cell lines.

Western blot validation of shRNA knockdowns:

Protein extracts were prepared by lysis of U-87 MG^{shSCM}, MG^{shATM}, MG^{shTDP1}, and MG^{shATM/TDP1} cells with buffer containing 50 mM Tris-HCl pH 7.5, 200 mM NaCl, 1% Tween-20 (vol/vol), 0.2% NP-40 (vol/vol), 1 mM NaF, 2 mM PMSF, 1 mM activated sodium vanadate, 50 mM β-glycerol phosphate, and Roche Complete Mini EDTA-free protease inhibitor cocktail. Lysis was performed on ice for 40 minutes, followed by centrifugation for 10 minutes at 13000 RPM and 4 °C. Quantification of protein lysates was performed by Bradford assay (Bio-Rad). The SpectraMax M5 spectrophotometer measured absorbance at 595 nm for each lysate, with subsequent analysis via SoftMax Pro v5.

25 µg of protein were combined with 4x loading dye containing 2.5% 2-mercaptoethanol (vol/vol). Samples were preheated at 95 °C for five minutes before being loaded onto precast Novex 4-12% Bis-Tris SDS polyacrylamide gels (Life Technologies). MG^{shSCM} lysates served as positive controls, with BLUelf Prestained Protein Ladder (GeneDirex) enabling determination of protein size. Electrophoresis for protein separation was performed for 100 minutes at 150 V in Novex Mini Gel Tanks (Life Technologies) containing NuPAGE MOPS SDS Running Buffer (Invitrogen; 50 mM MOPS, 50 mM Tris base, 0.1% SDS, 1 mM EDTA).

Proteins were electroblotted onto nitrocellulose membranes at 100 V for 90 minutes at 4°C in Criterion Blotter transfer apparatus (Bio-Rad) with NuPAGE Transfer Buffer (Invitrogen; 25 mM Bicine, 25 mM Bis-Tris, 1 mM EDTA). 5% milk in TBS-T (Tris buffered saline with 0.5% Tween 20) was used to block nitrocellulose membranes for one hour at room temperature. Blots were immunostained overnight at 4 °C with primary antibody to ATM (D2E2, rabbit, Cell Signaling), TDP1 (rabbit, Novus Biologicals), and beta-actin (rabbit, Sigma-Aldrich), each diluted 1:1000 in 5% milk in TBS-T. After 3x 15 minute washes in TBS-T, nitrocellulose membranes were incubated for one hour at room temperature with goat anti-rabbit horseradish peroxidase-conjugated secondary antibodies (Bio-Rad) diluted 1:5000 in 5% milk in TBS-T, followed by 3x 15 minute washes in TBS-T.

Protein detection was then carried out using Clarity Western ECL Substrate (Bio-Rad) and an ImageQuant LAS 500 imager (GE Healthcare). Ponceau staining of transferred membranes and primary antibody to beta-actin served as protein loading controls. ImageJ software was used to perform densitometric analysis of protein signals for quantification of the degree of ATM/TDP1 knockdown in cell samples.

Cell treatments:

In preparation for γ H2AX foci immunofluorescence and comet assay analysis, cells were treated either with γ -irradiation (2 Gy) or DMEM complete medium containing 0.5, 5, or 14 μ M camptothecin (Millipore) for 60 minutes at 37 °C. Cells were then either immediately harvested or incubated in drug-free medium at 37 °C to allow for DNA repair before proceeding with the assay.

For small molecule chemical inhibitor studies, cells were pre-incubated with medium containing 10 μ M ATMi (KU55933, EMD), 2 μ M PARPi (PJ34, EMD), 3 μ M DNA-PKi (NU7026, Sigma-Aldrich), or various combinations thereof for 30 minutes at 37 °C. Cells were then treated with camptothecin or γ -irradiation as described above, but in fresh medium also containing the appropriate chemical inhibitor(s) at the above concentrations.

γ H2AX foci immunofluorescence:

Cells were seeded on coverslips pre-sterilized in 100% ethanol and placed in 24 well plates. Following overnight incubation and appropriate treatments, cells were washed three times in PBS and then fixed in 0.5 mL of 4% PFA in 1x PBS for 9 minutes at room temperature. After another three washes in PBS, cells were permeabilized by incubation in 0.5 ml 0.5% Triton X-100 in PBS for 4 minutes.

Cells were again washed three times in PBS before being immunostained with anti- γ H2AX monoclonal primary antibodies (S139, rabbit, Cell Signaling, 1:500 dilution in 3% BSA in PBS) for one hour at room temperature in a humidified chamber. After washing three times in PBS, cells were incubated in donkey anti-rabbit fluorescent secondary antibodies (Alexa 555, Life Technologies, 1:500 dilution in 3% BSA in PBS), also for one hour in the humidified chamber.

Following a final three washes in PBS, coverslips were mounted onto optical slides via VECTASHIELD Mounting Medium containing DAPI. Slides were then visualized using a BX51 microscope at 400x magnification, with images captured by a CoolSNAPcf camera (Photometrics), allowing for quantification of γ H2AX foci. After assessment of at least 30 nuclei per sample, average γ H2AX foci values were calculated and graphed.

Alkaline comet assays:

U-87 MG cells were seeded at $\sim 3 \times 10^5$ cells/well in 24 well plates and incubated overnight to achieve $\sim 100\%$ confluency. After appropriate treatments, cells were washed three times in PBS, trypsinized, resuspended in DMEM complete medium, and centrifuged for 5 minutes at 1000 RPM and 4 °C. Cell pellets were resuspended in 1.5 mL ice-cold PBS to achieve a cell density $\sim 3 \times 10^5$ cells/mL, and transferred to pre-chilled black Eppendorf tubes to minimize light exposure. 150 μ l of resuspended cells were then mixed with an equal volume of 1.2% UltraPure low melting point agarose (Invitrogen; maintained at 42 °C in PBS) and immediately plated on Fully Frosted glass slides (Fisher) pre-coated with 0.6% UltraPure agarose (Invitrogen; maintained at 65 °C in PBS). All subsequent steps were performed in the dark at 4 °C.

Cell lysis was induced by immersion of slides in pre-chilled lysis buffer (2.5 M NaCl, 100 mM EDTA, 10 mM Tris-HCl, 1% Triton X-100 (vol/vol), 3% DMSO (vol/vol)) for 75 minutes. Slides were then washed in pre-chilled distilled water four times for a total of 10 minutes, before being immersed in pre-chilled electrophoresis buffer (1 mM EDTA, 50 mM NaOH, 1% DMSO (vol/vol)) for a 45 minute equilibration. Electrophoresis was conducted at 95 mA for 25 minutes in electrophoresis buffer.

Slides were neutralized with 0.4 M Tris-HCl (pH 7.0) for 60 minutes, and then stained for 5 minutes with SYBR Green dye (Sigma-Aldrich) diluted 1:5000 in 0.4 M Tris-HCl. The Comet Assay IV system (Perceptive Instruments) coupled to a BX51 microscope at 200x magnification was used to measure at least 100 comet tail moments per cell sample. Mean comet tail moments were assessed and graphed for each sample, and images were captured by the CoolSNAPcf camera (Photometrics).

WST-1 analysis of cell proliferation:

U-87 MG^{shScm}, MG^{shATM}, MG^{shTDP1}, and MG^{shATM/TDP1} cells were seeded in replicates of 16 in 96 well plates to achieve a cell quantity of 1000 cells/well, with a cell culture volume of 100 μ L/well. After a 24 hour incubation at 37 °C, 10 μ L of WST-1 cell proliferation reagent (Roche) was added to the first four replicates of each cell line. Following an additional 2 hour incubation at 37 °C, the SpectraMax M5 spectrophotometer was used to measure absorbance at 450 nm for each well, with subsequent analysis via SoftMax Pro v5. Mean absorbance for each sample was then calculated.

The above process was repeated successively for 48, 72, and 96 hour 37 °C incubations of seeded cells. Mean absorbance values for each time-point were then normalized with respect to the values derived for the 24 hour incubation of each sample, and the results were graphed.

WST-1 dose-response analysis of cytotoxicity:

U-87 MG^{shScm}, MG^{shATM}, MG^{shTDP1}, and MG^{shATM/TDP1} cells were seeded in replicates of 20 in 96 well plates in the same manner as for the cell proliferation analyses. Following a 24 hour incubation at 37 °C, growth medium was removed from each well and replaced with 100 μ L of fresh DMEM complete medium containing a range of CPT (10 μ M, 1 μ M, 0.1 μ M, 0.01 μ M, or 0.0 μ M), with four replicates of each cell line receiving each dose.

After a 48 hour incubation at 37 °C in the camptothecin-containing media, 10 μ L of WST-1 reagent was added to each well, and the cells were incubated for another 2 hours at 37 °C. The SpectraMax M5 spectrophotometer and SoftMax Pro v5 were used to measure absorbance at 450 nm for each well, with mean absorbance for each treatment also being calculated. Mean absorbance values for each treatment dose were then normalized with respect to the values derived for the 0.0 μ M treatments of each cell line (i.e. untreated), and the results were graphed.

Results:

Use of small molecule inhibitors of DNA repair pathways to chemoradiosensitize MG:

Small molecule inhibitors of ATM (KU55933, ATMi), DNA-PK (NU7026, DNAPKi), and PARP-1 (PJ34, PARPi) were used to coordinately inhibit these DNA repair enzymes and their respective DNA repair pathways in U-87, a well-defined grade IV MG. For example, co-treatment of cells with ATMi and PARPi resulted in co-inhibition of DNA DSB/SSBR. Similarly, co-treatment with ATMi and DNAPKi effectively co-inhibited different components of the DNA DSB/SSBR pathway. Using camptothecin and irradiation, and thus mimicking clinically-relevant MG chemoradiotherapeutic strategies[23, 24], DNA damage (comet and γ H2AX) assays were

performed to measure and compare the relative genotoxic effect of repair enzyme co-inhibition versus controls.

By means of γ H2AX foci immunofluorescence assays, we found that inhibition of specific DNA repair pathways increased the average relative number of γ H2AX foci in U-87 glioblastoma cells when co-treated with either camptothecin or ionizing radiation as compared to untreated control cells (Figs. 3, 4). γ H2AX assays utilize a fluorescent-tagged version of an antibody against phosphorylated histone H2AX, a protein normally associated with DNA in the cell nucleus, which becomes modified (phosphorylated) upon changes in DNA-protein structure resulting from genotoxic DNA strand breaks. H2AX phosphorylation initiates formation of a punctate nuclear pattern of γ H2AX foci which is subsequently visualized via epifluorescence microscopy, allowing for quantification of genotoxicity. Increased γ H2AX signals correlate with higher cellular DNA damage[25]. Although a marked increase in γ H2AX foci was seen upon treatment of cells in which only one DNA repair molecule was inhibited, the greatest effect was demonstrated by co-inhibiting pairs of repair enzymes, such as both ATM and PARP-1 (ATMi/PARPi), suggesting that this bimodal co-inhibition strategy is most effective at sensitizing MG cells to genotoxic therapeutics. For example, chemosensitization through co-inhibition of ATM and PARP-1 resulted in a 104% increase in average γ H2AX foci per cell as compared to control cells treated with camptothecin. Co-inhibition of ATM and DNA-PK (ATMi/DNA-PKi) produced a 111% increase in average foci.

Immunofluorescence assays also revealed that this increase in γ H2AX foci through repair enzyme co-inhibition relative to control cells is maintained for extended periods of time post-treatment (Fig. 4). Cells treated with ionizing radiation were left for differing lengths of time in order to allow repair of the DNA damage they had incurred. While control cells without repair inhibitors saw a significant amount of repair between 15 minutes and three hours post-irradiation, as exemplified by a decrease in number of γ H2AX foci, cells co-treated with repair pathway inhibitors showed reduced DNA repair. Once again, this difference was most conspicuous for cells in which pairs of repair molecules were co-inhibited, i.e. both ATM and PARP-1, ATM and DNA-PK, or DNA-PK and PARP-1.

Alkaline comet assay analysis also showed that an analogous bimodal strategy increased the number of unrepaired DNA breaks versus control cells as demonstrated by higher comet tail moment values when U-87 cells were co-treated with ATMi/PARPi and camptothecin (Fig. 5). Similar to γ H2AX foci experiments, comet assays are a means of quantifying cellular DNA damage through fluorescent microscopy performed on cells treated with genotoxic agents. The strand breaks produced by camptothecin result in loss of DNA supercoiling and, upon electrophoresis, formation of a nuclear tail of fragmented damaged DNA resembling a comet. Comparison of the comet tail to the nuclear head allows for derivation of the comet tail moment, which is then used as a measurement of genotoxicity, where higher tail moment values correspond to greater DNA damage[26]. Compared to control cells, larger comet tail moments were observed for U-87 cells co-treated with individual inhibitors of DNA repair, and the effect was augmented further upon co-inhibition of both ATM and PARP-1.

Analysis of the coordinate anti-cancer effect of DNA repair inhibition via genetic techniques:

In addition to the experiments performed on cells treated with chemical inhibitors of DNA repair molecules, assays were also conducted on U-87 MG cells in which human ATM and TDP1 had been knocked down using lentivirus-delivered short-hairpin RNAs (shRNAs). Puromycin selection was used to generate stable shScrambled (MG^{shScm}), shATM (MG^{shATM}), shTDP1

(MG^{shTDP1}), and shATM/shTDP1 (MG^{shATM/TDP1}) cell lines. Validation of the efficacy of the shRNAs in establishing these knockdowns was confirmed by western analysis (Fig. 6).

As with the repair molecule inhibitor studies, γ H2AX immunofluorescence assays carried out on U-87 knockdown cell lines showed that DNA repair pathway inhibition increased average numbers of γ H2AX foci and DNA damage when compared to MG^{shScm} control cells (Fig. 7). While an increase in CPT-associated DNA damage (γ H2AX foci), was seen in cells in which either ATM or TDP1 alone had been inhibited, the greatest genotoxic effect was observed in the double knockdown MG^{shATM/TDP1} cells, paralleling the results of the ATMi/PARPi small molecule inhibitor studies.

Finally, WST-1 cell proliferation and cytotoxicity assays performed on these shRNA U-87 cell lines revealed decreased proliferation rate and increased cytotoxic response to camptothecin in ATM/TDP1 knockdown cells compared to controls (Figs. 8, 9). Proliferating cells incubated with WST-1 reagent catalyze its reduction to formazan in proportion to cellular metabolic activity. Average sample absorbance can then be measured by spectrophotometry, providing a relative indicator of cell growth[27]. The MG^{shATM/TDP1} double knockdown cells displayed a significant reduction in growth over the course of four days compared to the MG^{shScm} control cells (2-fold, Fig. 8). Furthermore, the double knockdown cells demonstrated greatly reduced viability upon treatment with camptothecin compared to controls, and this increased cytotoxicity was observed consistently over a spectrum of chemotherapeutic doses (Fig. 9).

Discussion:

In this study, I have found that coordinate inhibition of ATM and the DNA SSBR pathway is an effective method to chemoradiosensitize glioblastoma multiforme cells and induce pronounced genotoxic damage. Furthermore, using a genetic approach, I show that specific co-inhibition of ATM and TDP1 can achieve this sensitization effect. These data are consistent with our previous findings that dual inhibition of ATM and TDP1 mediated DNA DSB/SSBR result in combined sensitivity to Top1-mediated damage in proliferating neuroprogenitor cells while sparing non-proliferating neural cells. Similarly, as MG are a highly proliferating tumour cell in a relatively quiescent and post-mitotic environment (neurons/brain), by means of this strategy, we can augment chemoradiotherapy induced DNA damage and enhance tumour cell death at lower drug doses, thus potentiating therapy while potentially reducing off-target effects and patient side-effects.

The amplification of genotoxicity upon inhibition of ATM or TDP1 demonstrated by γ H2AX immunofluorescence assays performed on the MG^{shATM} and MG^{shTDP1} U-87 cell lines suggests that these repair enzymes are integral components of the MG response to damage induced by camptothecin. Since the basis for the use of camptothecin in the treatment of MG is its promotion of Top1-cc survival, and thus induction of DNA SSBs[28], failure of MG to mount as prolific a damage repair response following inhibition of ATM or TDP1 indicates that these enzymes are key to proper resolution of Top1-cc's and/or the associated DNA breaks. This conclusion is compatible with the current understanding of the actions of ATM and TDP1 in the nervous system: 1. ATM-mediated ubiquitination/sumoylation and proteasomal degradation and turnover of Top1[30] and, 2. TDP1-mediated processing of Top1-cc formation through cleavage of the 3'-end covalent Top1-DNA complex phosphodiester bond[29].

The most striking chemosensitizing effect demonstrated by the γ H2AX assays conducted on the shRNA cell lines was observed not in the MG^{shATM} or MG^{shTDP1} single knockdown U-87 cells, but rather in the MG^{shATM/TDP1} double knockdown cell line. This is a significant finding considering it

has been previously shown that ATM inhibition or TDP1 inhibition alone causes no overt neuropathology in mice, suggesting that there is a DNA damage threshold that must be met in order to produce observable pathologic consequences, and potentially limiting the therapeutic advantage of individual repair molecule inhibition[31]. The bimodal strategy of ATM and TDP1 co-inhibition undertaken in my study is a promising method to overcome this limit, potentially increasing DNA damage sufficiently to surpass this damage threshold and notably enhance therapeutic efficacy.

My WST-1 cell proliferation assay data lend credence to the encouraging nature of this bimodal treatment strategy, as they indicate that ATM and TDP1 co-inhibition is capable not only of increasing tumour cell DNA damage, but also of markedly amplifying MG cell death in response to a particular dose of chemotherapy. This is exemplified by my finding that the LD50 for CPT-treated MG cells (MG^{shScm}) is greater than 280-fold higher than that of ATM/TDP1 co-inhibited MG cells (MG^{shATM/TDP1}). The fact that co-inhibition is resulting in both a magnification of DNA damage and a corresponding enhancement of cytotoxicity implies that ATM/TDP1 co-inhibition is lowering the genotoxic threshold required for a clinically significant improvement in therapeutic response. Furthermore, these findings directly suggest that ATM/TDP1 co-inhibition is capable of chemosensitizing MG cells to a sufficient therapeutic extent that precludes the need for deleteriously high doses of chemotherapy. My strategy would suggest that smaller drug doses may produce a better therapeutic response in ATM/TDP1 co-inhibited MG than the doses normally used in the absence of repair molecule co-inhibition. Furthermore, I find that untreated MG^{shATM/TDP1} cells also exhibit proliferation defects in comparison to control cells. Even without administration of chemotherapy, MG cells in which ATM and TDP1 were co-inhibited displayed a defective growth pattern. This suggests that repair pathway inhibition has the ability to prevent adequate repair of the base level intrinsic DNA damage present in untreated tumour cells in addition to damage induced by exogenous treatment modalities, demonstrating the therapeutic potential of repair inhibitors in their own right.

Synthetic lethality refers to cytotoxicity due to disruption of two or more genes for which disruption of either individual gene alone does not result in cell death[32]. Importantly, previous data has shown that the synthetic lethality between ATM and TDP1 is due specifically to nervous system defects[31]. This finding, in combination with the fact that the vast majority of Top1-cc induced DNA damage is in the form of SSBs, which almost exclusively present as neuropathology[15], makes the study of ATM and TDP1 and the effect of their co-inhibition on SSBR, especially relevant to brain cancers in particular, such as MG. It is noteworthy that as many as 20% of all tumours are found to contain mutations in *ATM*, thus affording an opportunity to integrate the use of TDP1 inhibitors as a synthetic lethal treatment strategy[33].

The results of assays performed on MG cells in which ATM and TDP1 were knocked down using shRNAs were corroborated by the findings of assays conducted on U-87 cells treated with various combinations of small molecule chemical inhibitors of DNA repair molecules, again indicating that dual repair enzyme co-inhibition is most effective at sensitizing MG to the effects of treatment. One of the most powerful combinations of inhibitors was the ATMi/PARPi pairing, producing a pronounced increase in genotoxic damage compared to control cells in response to both chemotherapy and ionizing radiation, as demonstrated by γ H2AX immunofluorescence and comet assay analysis. This ATMi/PARPi inhibitor pairing is of particular interest in relation to the ATM and TDP1 shRNA studies, as it was the combination anticipated to most closely mimic the effects of ATM/TDP1 double knockdown. Although their specific actions are different, TDP1 and PARP-1 are both key molecules in the SSBR pathway. PARP-1 is located upstream of TDP1, so its inhibition should theoretically prevent proper functioning of downstream SSBR enzymes, including TDP1[22]. The findings of this study substantiate this theory, suggesting that

ATM/TDP1 double knockdown and ATM/PARP-1 co-inhibition have analogous chemoradiosensitizing effects on MG, enhancing genotoxicity to a comparable degree. Furthermore, they imply that shRNAs and small molecule inhibitors of DNA repair enzymes are equally effective sensitizing agents for the treatment of MG.

The persistence of high levels of γ H2AX foci in irradiated cells co-treated with two small molecule inhibitors of DNA repair enzymes three hours post-treatment suggests a drastic reduction in peak DNA damage repair kinetics in comparison to control cells. This illustrates an additional effect of repair pathway co-inhibition on MG cells. Not only does repair enzyme co-inhibition chemoradiosensitize MG by increasing the absolute amount of DNA damage incurred by therapy, but it also maintains these high damage levels for extended time periods, impeding both the effectiveness and rate of tumour DNA repair efforts.

In conclusion, my study demonstrates that co-inhibition of DNA repair chemoradiosensitizes glioblastoma tumour cells to conventional therapy, thus offering a more refined and targeted cancer treatment strategy which may lead to improved patient survival and quality-of-life. By lowering the genotoxic threshold of brain tumour cells through inhibition of redundant repair pathways, therapy can be administered in smaller doses so as to limit chemotoxic side effects and damage to non-cancer cells. With the availability of known chemical inhibitors of DNA repair, there is scope to introduce these agents into existing cancer therapy treatment regimens in future clinical trials.

Acknowledgements:

I gratefully acknowledge the support entirely or in part by one or all of the following B.Sc. (Med) sponsors: H.T. Thorlakson Foundation, Dean Faculty of Medicine, St. Boniface Research Foundation, Manitoba Health Research Council, Manitoba Institute of Child Health, Kidney Foundation of Manitoba, Leukemia and Lymphoma Society of Canada, CancerCare Manitoba Foundation, Manitoba Medical Service Foundation, Associate Dean (Research) Faculty of Medicine, Heart and Stroke Foundation, Health Sciences Centre Research Foundation, University of Manitoba and a grant from the Canadian Institutes of Health Research.

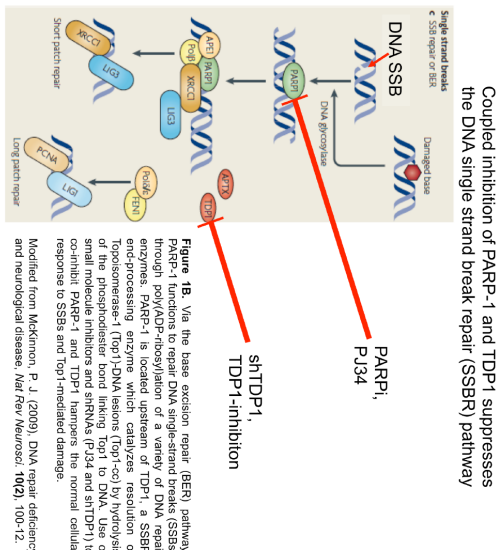
I would also like to acknowledge the support of the members of the Katyal lab, including Dr. Sachin Katyal, Ali Saleh, Bozena Kuzio, Daniel Huang, Elise Labossiere, Rahmat Rahman, Asha Sinha, and Rajas Tipnis, as well as the lab of Spencer Gibson for providing cell lines.

References:

1. Louis, D. N., Ohgaki, H., Wiestler, O. D., Cavenee, W. K., Burger, P. C., Jouvett, A., Scheithauer, B. W. & Kleihues, P. (2007) The 2007 WHO classification of tumours of the central nervous system, *Acta Neuropathol.* **114**, 97-109.
2. Goodenberger, M. L. & Jenkins, R. B. (2012) Genetics of adult glioma, *Cancer Genet.* **205**, 613-21.
3. Stupp, R., Mason, W. P., van den Bent, M. J., Weller, M., Fisher, B., Taphoorn, M. J., Belanger, K., Brandes, A. A., Marosi, C., Bogdahn, U., Curschmann, J., Janzer, R. C., Ludwin, S. K., Gorlia, T., Allgeier, A., Lacombe, D., Cairncross, J. G., Eisenhauer, E. & Mirimanoff, R. O. (2005) Radiotherapy plus concomitant and adjuvant temozolomide for glioblastoma, *N Engl J Med.* **352**, 987-96.
4. Wen, P. Y. & Brandes, A. A. (2009) Treatment of recurrent high-grade gliomas, *Curr Opin Neurol.* **22**, 657-64.
5. Scott, J. N., Rewcastle, N. B., Brasher, P. M., Fulton, D., Hagen, N. A., MacKinnon, J. A., Sutherland, G., Cairncross, J. G., Forsyth, P. (1998) Long-term glioblastoma multiforme survivors: a population-based study, *Can J Neurol Sci.* **25**, 197-201.
6. Choucair, A. K., Levin, V. A., Gutin, P. H., Davis, R. L., Silver, P., Edwards, M. S., Wilson, C. B. (1986) Development of multiple lesions during radiation therapy and chemotherapy in patients with gliomas, *J Neurosurg.* **65**, 654-8.
7. Mason, W. P., Del Maestro, R., Eisenstat, D., Forsyth, P., Fulton, D., Laperriere, N., Macdonald, D., Perry, J., Thiessen, B. (2007) Canadian recommendations for the treatment of glioblastoma multiforme, *Curr Oncol.* **14(3)**, 110-117.
8. Beretta, G. L., Cossa, G., Gatti, L., Zunino, F. & Perego, P. (2010) Tyrosyl-DNA phosphodiesterase 1 targeting for modulation of camptothecin-based treatment, *Curr Med Chem.* **17**, 1500-8.
9. Dexheimer, T. S., Antony, S., Marchand, C. & Pommier, Y. (2008) Tyrosyl-DNA phosphodiesterase as a target for anticancer therapy, *Anticancer Agents Med Chem.* **8**, 381-9.
10. Kaelin, W. G. Jr. (2005) The concept of synthetic lethality in the context of anticancer therapy, *Nat Rev Cancer.* **5**, 689-98.
11. Jorgensen, T. J. (2009) Enhancing radiosensitivity: targeting the DNA repair pathways, *Cancer Biol Ther.* **8(8)**, 665-70.
12. Caldecott, K. W. (2008) Single-strand break repair and genetic disease, *Nat Rev Genet.* **9**, 619-31.
13. McKinnon, P. J. & Caldecott, K. W. (2007) DNA strand break repair and human genetic disease, *Annu Rev Genomics Hum Genet.* **8**, 37-55.
14. McKinnon, P. J. (2009) DNA repair deficiency and neurological disease, *Nat Rev Neurosci.* **10(2)**, 100-12.
15. Katyal, S., McKinnon, P. J. (2009) Mouse models of DNA double strand break repair deficiency and cancer, *The DNA Damage Response: Implications on Cancer Formation and Treatment.* 285-305.
16. Gurley, K. E., Kemp, C. J. (2001) Synthetic lethality between mutation in Atm and DNA-PK_{cs} during murine embryogenesis, *Curr Biol.* **11**, 191-4.
17. Caldecott, K. W. (2008) Single-strand break repair and genetic disease, *Nature Rev Genet.* **9**, 619-31.
18. Wang, J. C. (2002) Cellular roles of DNA topoisomerases: a molecular perspective, *Nat Rev Mol Cell Biol.* **3**, 430-40.
19. Katyal S., El-Khamisy, S. F., Russell, H. R., Li, Y., Ju, L., Caldecott, K. W., McKinnon, P. J. (2007) TDP1 facilitates chromosomal single-strand break repair in neurons and is neuroprotective in vivo, *EMBO J.* **26(22)**, 4720-31.

20. Katyal, S., Lee, Y. S., Nitiss, K., Downing, S., Li, Y., Shimada, M. Zhao, J., Russell, H.R., Nitiss, J.L., McKinnon, P. J. (2014) Topoisomerase-1 cleavage complexes define a novel pathogenic lesion in neurodegenerative syndromes characterized by genome instability, *Nature Neurosci (accepted)*.
21. El-Khamisy, S. F., Katyal, S., Patel, P., Ju, L., McKinnon, P. J., Caldecott, K. W. (2009) Synergistic decrease of DNA single-strand break repair rates in mouse neural cells lacking both Tdp1 and aprataxin, *DNA Repair*. **8**, 760-66.
22. El-Khamisy, S. F., Saifi, G. M., Weinfeld, M., Johansson, F., Helleday, T., Lupski, J. R., Caldecott, K. W. (2005) Defective DNA single-strand break repair in spinocerebellar ataxia with axonal neuropathy-1, *Nature*. **434**, 108-13.
23. Levy, A. S., Meyers, P. A., Wexler, L. H., Jakacki, R., Angiolillo, A., Ringuette, S. N., Cohen, M. B. & Gorlick, R. (2009) Phase 1 and pharmacokinetic study of concurrent carboplatin and irinotecan in subjects aged 1 to 21 years with refractory solid tumors, *Cancer*. **115**, 207-16.
24. Meco, D., Di Francesco, A. M., Cusano, G., Bucci, F., Pierri, F., Patriarca, V., Torella, A. R., Pisano, C. & Riccardi, R. (2012) Preclinical evaluation of the novel 7-substituted camptothecin Namitecan (ST1968) in paediatric tumour models, *Cancer Chemother Pharmacol*. **70**, 811-22.
25. Redon, C. E., Dickey, J. S., Bonner, W. M., Sedelnikova, O. A. (2009) γ -H2AX as a biomarker of DNA damage induced by ionizing radiation in human peripheral blood lymphocytes and artificial skin, *Adv Space Res*. **43(8)**, 1171-78.
26. Collins, A. R. (2004) The comet assay for DNA damage and repair: principles, applications, and limitations, *Mol Biotechnol*. **26(3)**, 249-61.
27. Berridge, M. V., Herst, P. M., Tan, A. S. (2005) Tetrazolium dyes as tools in cell biology: new insights into their cellular reduction, *Biotechnol Annu Rev*. **11**, 127-52.
28. Rodriguez-Galindo, C., Radomski, K., Stewart, C. F., Furman, W., Santana, V. M., Houghton, P. J. (2000) Clinical use of topoisomerase I inhibitors in anticancer treatment, *Med Pediatr Oncol*. **35**, 385-402.
29. Pouliot, J. J., Yao, K. C., Roberston, C. A., Nash, H. A. (1999) Yeast gene for a Tyr-DNA phosphodiesterase that repairs topoisomerase I complexes, *Science*. **286**, 552-5.
30. Lin, C. P., Ban, Y., Lyu, Y. L., Desai, S. D., Liu, L. F. (2008) A ubiquitin-proteasome pathway for the repair of topoisomerase I-DNA covalent complexes, *J Biol Chem*. **283(30)**, 21074-83.
31. Katyal, S., Lee, Y., Nitiss, K. C., Downing, S. M., Li, Y., Shimada, M., Zhao, J., Russell, H. R., Petrini, J. H. J., Nitiss, J. L., McKinnon, P. J. (2014) Aberrant topoisomerase-1-DNA lesions are pathogenic in neurodegenerative genome instability syndromes, *Nat Neurosci*. **17(6)**, 813-21.
32. Tucker, C. L., Fields, S. (2003) Lethal combinations, *Nat Genet*. **35(3)**, 204-5.
33. Stagni, V., Oropallo, V., Fianco, G., Antonelli, M., Cina, I., Barila, D. (2014) Tug of war between survival and death: exploring ATM function in cancer, *Int J Mol Sci*. **15(4)**, 5388-409.

Figures:



Abbreviations:
MG, malignant glioma; ATM, Ataxia telangiectasia mutated; DNA-PKcs, DNA-PK catalytic subunit; PARP-1, Poly(ADP-ribose) polymerase-1; TDP1, Tyrosyl-DNA phosphodiesterase 1; SSB, single strand break; SSBR, single strand break repair; DSB, double strand break; DSBR, double strand break repair; KUS5933/ATMi, small molecule inhibitor of ATM; NU7026/DNA-PKi, small molecule inhibitor of DNA-PK; P334/PARPi, small molecule inhibitor of PARP; shRNA, short-hairpin RNA; shATM, shRNA knockdown of ATM; shTDP1, shRNA knockdown of TDP1; shScm, non-target scrambled shRNA; MG^{shATM}, MG cell line with shATM; MG^{shTDP1}, MG cell line with shTDP1; MG^{shScm}, MG cell line with shScm; CPT, camptothecin; IR, ionizing radiation; NHEJ, non-homologous end-joining; BER, base excision repair; Top1, Topoisomerase 1; Top1-cc, Topoisomerase 1 cleavage complex; SCAN1, spinocerebellar ataxia with axonal neuropathy-1; MRN, Mre11/Nbs1/Rad50; XRCC1, X-ray repair cross-complementing protein 1

Co-inhibition of ATM and DNA-PKcs suppresses the DNA double-strand break repair (DSBR) pathway

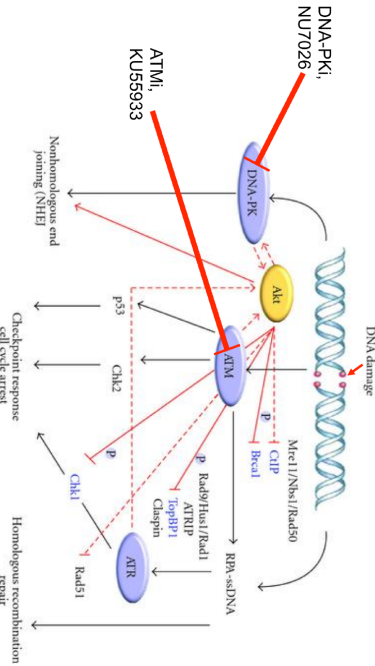
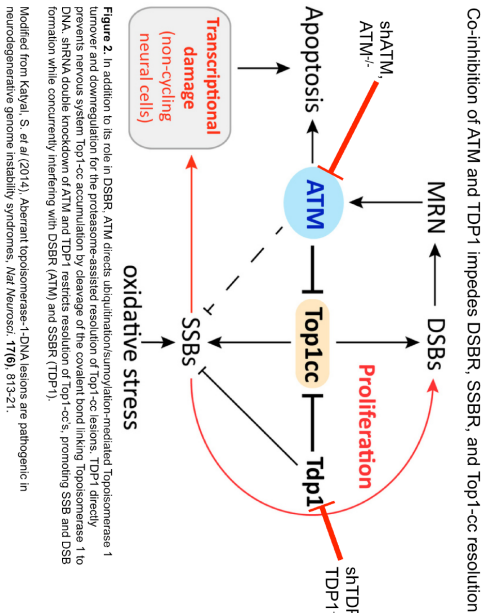


Figure 1A. ATM forms the apex of the DNA DSBR cascade, orchestrating a damage response that ultimately results in apoptosis or checkpoint activation for cell cycle arrest and DNA repair by selective substrate serine/threonine phosphorylation. DNA-PKcs protects the broken ends of DSBs while simultaneously recruiting additional repair factors to catalyze substrate strand ligation via the NHEJ pathway. Co-inhibition of ATM and DNA-PK (ATMi and DNA-PKi) with small molecule inhibitors (KUS5933 and NU7026) interferes with normal signal transduction for repair of DSBs.

Modified from Xu, N. et al (2012). Ataxia: A double-edged sword in cell proliferation and genome stability. *J. Oncol*, 2012, 951724.



yH2AX foci immunofluorescence assay:
CPT chemosensitization through DNA repair enzyme co-inhibition by small molecule inhibitors

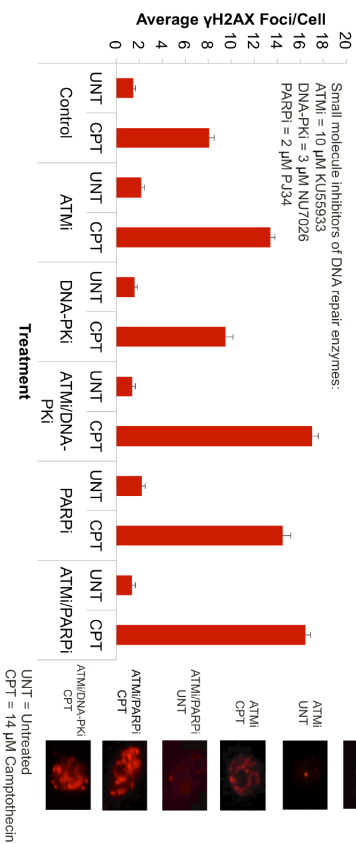


Figure 3A: Average yH2AX foci per cell as a measure of DNA damage. Glioblastoma genotoxicity due to camptothecin treatment as a result of inhibition of individual DNA repair enzymes using small molecule inhibitors. This effect is significantly enhanced upon co-inhibition of pairs of DNA repair molecules, i.e. ATM+DNA-PKcs and ATM+PARP-1.

yH2AX foci immunofluorescence assay: Radiosensitization through DNA repair enzyme co-inhibition by small molecule inhibitors

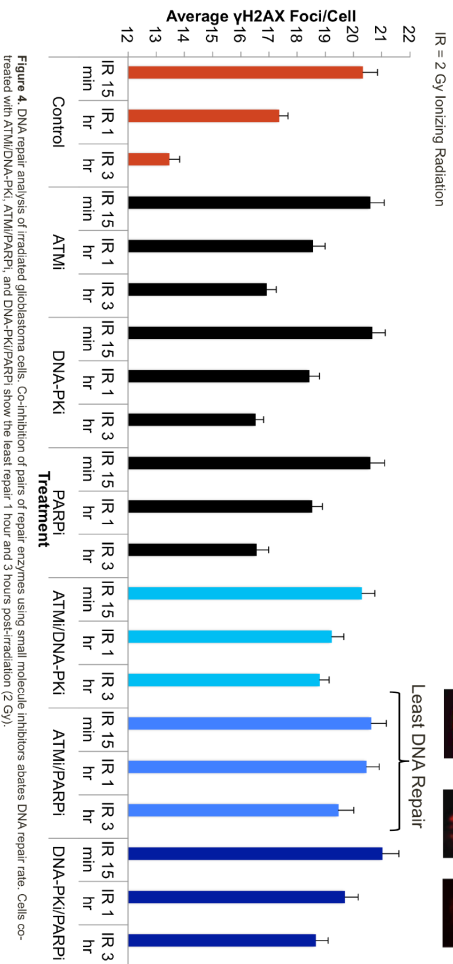


Figure 4: DNA repair analysis of irradiated glioblastoma cells. Co-inhibition of pairs of repair enzymes using small molecule inhibitors ablates DNA repair rate. Cells co-treated with ATM/DNA-PKi, ATM/PARPi, and DNA-PKi/PARPi show the least repair 1 hour and 3 hours post-irradiation (2 Gy).

yH2AX foci immunofluorescence assay:
CPT chemosensitization through DNA repair enzyme co-inhibition by small molecule inhibitors

Treatment Comparison	Increase in Average yH2AX Foci/cell
Control to ATMi	66%
Control to DNA-PKi	18%
Control to PARPi	79%
Control to ATMi/DNA-PKi	111%
Control to ATMi/PARPi	104%
ATMi to ATMi/DNA-PKi	27%
DNA-PKi to ATMi/DNA-PKi	79%
ATMi to ATMi/PARPi	23%
PARPi to ATMi/PARPi	14%

Figure 3B: Average yH2AX foci per cell as a measure of DNA damage. Glioblastoma genotoxicity due to camptothecin increases as a result of inhibition of individual DNA repair enzymes using small molecule inhibitors. This effect is significantly enhanced upon co-inhibition of pairs of DNA repair molecules, i.e. ATM+DNA-PKcs and ATM+PARP-1.

Alkaline comet assay:
CPT chemosensitization through DNA repair enzyme co-inhibition by small molecule inhibitors

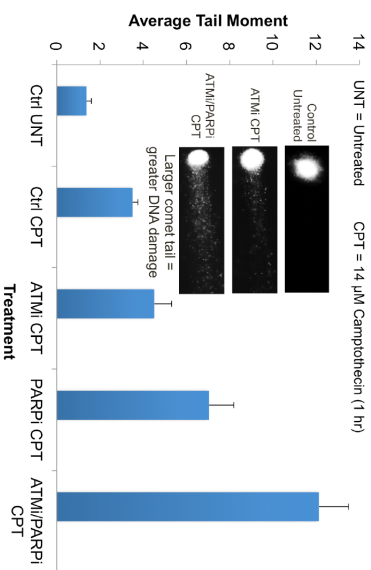


Figure 5: Average nuclear DNA comet tail moment as a measure of genotoxicity. Co-inhibition of DNA repair enzymes enhances DNA damage incurred by CPT treatment. Cells co-treated with ATM/ PARPi display the greatest genotoxicity.

Western blot validation of shRNA repair enzyme knockdowns

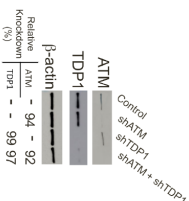


Figure 6. Validation of ATM and TDP1 single and double knockdown in glioblastoma cells. Western blot analysis of ATM (ATM), TDP1 (TDP1), and β-actin (β-actin) in shATM, shTDP1, and shATM + shTDP1 cells. Knockdowns were consistently greater than 90% relative to the shSCM controls. β-actin served as a protein loading control.

yH2AX foci immunofluorescence assay: CPT Chemosensitization through DNA repair enzyme co-inhibition by shRNA knockdown

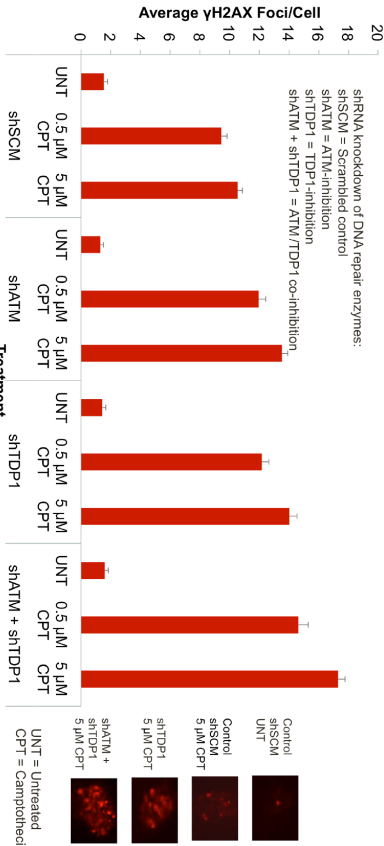


Figure 7. Average yH2AX foci per cell as a measure of DNA damage. Glioblastoma cells show further enhanced CPT-mediated DNA damage as a result of DNA repair enzyme co-inhibition.

WST-1 cell proliferation assay: Impairment of cell proliferation through repair enzyme co-inhibition by shRNA knockdown

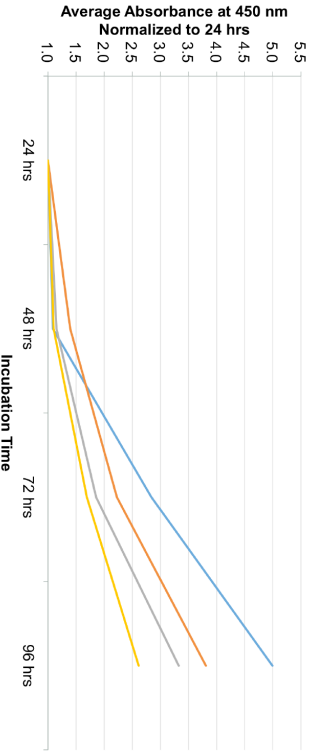


Figure 8. Average absorbance at 450 nm as a measure of cell proliferation. Glioblastoma cell proliferation rate decreases following shRNA knockdown of ATM or TDP1. Dual ATM/TDP1 co-inhibition in shATM/shTDP1 double knockdown cells results in further impairment of MG cell growth.

WST-1 camptothecin dose-response cytotoxicity assay: Increased cytotoxicity via DNA repair enzyme co-inhibition

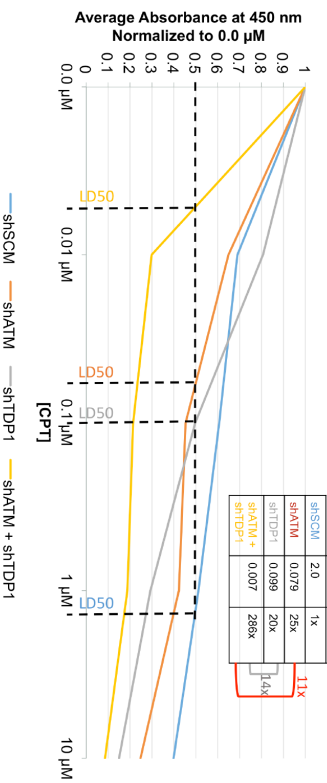


Figure 9. Average absorbance at 450 nm as a measure of cell viability. Glioblastoma cells show increased sensitivity to CPT following shRNA knockdown of ATM or TDP1. Dual ATM/TDP1 co-inhibition results in further impairment of cell viability, with a marked reduction in LD50 compared to shSCM control cells (~300-fold). CPT-mediated cytotoxicity is synergistically sensitized by 16-fold increased sensitivity compared to individual knockdowns, indicating that a co-inhibition strategy synergistically sensitizes MG to CPT.